PCCP

PAPER

View Article Online
View Journal | View Issue

Check for updates

Cite this: *Phys. Chem. Chem. Phys.*, 2018, **20**, 21051

Circularly polarised fluorescence and phosphorescence calculations on organic molecules using the approximate coupled-cluster model CC2†

Chetana Badala Viswanatha, *[a] Benjamin Helmich-Paris [b] and Christof Hättig [a]

Received 28th May 2018,
Accepted 23rd July 2018

DOI: 10.1039/c8cp03385d

rsc.li/pccp

We report the first calculations of rotational strengths for circularly polarised phosphorescence at the coupled cluster level. The rotational strengths for circular dichroism (CD), circularly polarised fluorescence (CPF) and circularly polarised phosphorescence (CPP) were calculated for β,γ-enones and ketones with conjugated double bonds using the CC2 model. To compute spin-forbidden CPP, spin–orbit coupling with perturbation theory is employed within a response theory framework (SOC-PT-CC2). For closed-shell molecules containing only light elements, a spin-free formalism is used to treat the singlet–triplet transitions. It is verified that the simplification obtained in the spin-free formulation from the Wigner–Eckart theorem for spin-forbidden oscillator strengths is also valid for the rotational strengths. Our implementation utilises the resolution of identity (RI) approximation for two-electron integrals which facilitates applications to larger molecules. In the current study, the rotational strength for spin-forbidden circularly-polarised phosphorescence was calculated for a chiral aromatic system, *S*-DMBDA, containing 44 atoms.

Published on 26 July 2018. Downloaded by Ruhr Universitat Bochum on 12/22/2018 1:42:38 PM.

1 Introduction

A striking example of circularly polarised luminescence (CPL) in nature was reported in 1980.[1] The left and right lanterns of live larvae of fireflies were found to emit circularly polarised light with opposite handedness. Although CPL measurements on chiral samples date back to 1948,[2] first principle calculations of vibrationally resolved CPL were only reported in 2010 using time-dependent density functional theory (TD-DFT).[3] The possible use of circular dichroism (CD) and CPL spectra combined with theoretical calculations as a probe for conformational changes upon electronic excitation has been demonstrated since 1974.[4]

Circular dichroism is the differential absorption of left and right circularly polarised light by optically active compounds.[5] Spontaneous and induced emission of circularly polarised light is expected to occur in optically active compounds because the theoretical expressions for both light absorption and emission contain the same molecular quantities.[6] In a study by Emeis and Oosterhoff,[6] circular polarisation was shown to occur both in fluorescence and phosphorescence. CPL is the emission analogue of CD and thus measures the differential emission of left and right circularly polarised light by chiral luminescent systems.[7]

The difference in absorption or emission coefficients between left and right circularly polarised light is proportional to the pseudoscalar rotational strength for the transition from the ground to an excited state in randomly oriented molecules.[8] In linear response theory, the rotational strength is obtained from residues of the linear response function.[9,10] Coupled cluster response calculations of natural chiroptical spectra were reported in 1999[10] using the coupled cluster singles and doubles (CCSD) model.

In circularly polarised fluorescence (CPF) of closed-shell molecules the excited state is a singlet state and the transition is spin-allowed to the singlet ground state.[11] The CPL intensity is also proportional to the rotational strength between the excited state and the ground state. The only difference for computations is that the rotational strengths are evaluated at the equilibrium structure of the excited state opposed to the ground state structure needed for CD.[8] CPF has also been investigated with EOM-CCSD.[12] A review article[13] on CPL asserts that TD-DFT is the most widely used method for

[a] *Lehrstuhl für Theoretische Chemie, Ruhr Universität Bochum, D-44780, Bochum, Germany. E-mail: BadalaViswanatha@rub.de, Christof.Haettig@rub.de*
[b] *Max-Planck-Institut für Kohlenforschung, Kaiser-Wilhelm-Platz 1, D-45470 Mülheim an der Ruhr, Germany. E-mail: helmichparis@kofo.mpg.de*

† Electronic supplementary information (ESI) available: Proof of the WET for the lowest-order SOC-induced rotational strengths. See DOI: 10.1039/c8cp03385d

Published on 26 July 2018. Downloaded by Ruhr Universitat Bochum on 12/22/2018 1:42:38 PM.

computing and interpreting CPL spectra for small to mid-sized molecules.

In circularly polarised phosphorescence (CPP) of closed-shell molecules the excited state is a triplet state and the transition to the singlet ground state is spin-forbidden in non-relativistic quantum mechanics.[11] A direct computation of spin-forbidden transition moments requires two- (or four-) component relativistic calculations to include the spin–orbit coupling which breaks the spin symmetry of non-relativistic quantum mechanics. A relativistic calculation for example can be performed using the exact two-component (X2C) ansatz.[14,15] This is still expensive for correlated wave function methods.

The SOC effects are small for molecules with light elements and an alternative cost-efficient way to account for spin–orbit coupling is then to use perturbation theory (SOC-PT). This has the additional advantage that it can for closed-shell molecules be combined with a spin-free formalism,[16] which was recently implemented for the approximate coupled cluster singles and doubles method CC2 for SOC-induced dipole transition moments.[17] An explicitly spin-coupled basis for singlet and triplet operators was used and thereby a spin–orbital treatment avoided for closed shell systems. For RI-CC2 the spin-free formalism is by a factor of 2–3 cheaper than the spin–orbital formalism. The SOC-PT ansatz within the response theory framework has also been implemented earlier at the MCSCF,[18] TDDFT[11] and CCSD[19] level for oscillator strengths of singlet–triplet transitions.

CC2 is an economical alternative to CCSD which is capable of treating larger molecules, but still gives excitation energies for single excitation dominated transitions with about the same accuracy. Also, CC2 can be very efficiently combined with the resolution-of-the-identity (RI) approximation for the electron repulsion integrals which reduces the computational costs further and makes RI-CC2 capable of handling molecules 2–3 times larger than conventional CC2, while the errors from the RI approximation are orders of magnitudes smaller than the inherent errors of the CC2 method. The RI-CC2 implementation[17] of phosphorescence lifetimes using SOC-PT is roughly an order of magnitude faster than a two-component relativistic RI-CC2 calculation. The accuracy of phosphorescence lifetimes for the lowest triplet states in halogen hydrides did not differ by more than 50% from those obtained with X2C-CC2. However, for heavier elements like bromine in the higher nearly degenerate states the SOC-PT-CC2 was a poor approximation because the spin–orbit correction to the excitation energies was of the same order of magnitude as the energy differences between electronic states in a one-component calculation. In the current work, the molecules under study contain only light elements: C, N, O, H.

Molecular systems where phosphorescence contributions to emission spectra become important pose a challenge for theoretical calculations.[13] So far, a theoretical and computational protocol seems to have been developed only for TD-DFT and applied to some chiral enones and diketones.[11] No experimental data has been reported for the CPP strengths of these molecules.

The current study aims at establishing the working protocol for computing CPP with CC response theory in combination with SOC-PT so that the computational advantages of a spin-free formalism can be exploited. We verify that the simplification obtained from the Wigner–Eckart theorem for the SOC-induced oscillator strengths in phosphorescence,[17] which is a scalar quantity, is also valid for the pseudoscalar rotational strengths needed for circularly polarised phosphorescence. Another objective of this study is to verify that the gauge-origin invariance of the rotational strengths for CPP and spin-forbidden CD is conserved in the velocity gauge formulation for CC response theory as it is the case for the rotational strengths for normal (*i.e.* spin-allowed) circular dichroism.[20]

In addition to the molecules studied in ref. 11 at the TDDFT level, we investigated in this work for the first time also a the CPP of larger metal-free chiral aromatic system for which recently experimental data for room-temperature persistent CPP became available.[21]

2 Theoretical background

The effective one-electron spin–orbit coupling operator V^{SOC} can be expressed in the spin-tensor form as:

$$V^{\mathrm{SOC}} = \frac{1}{2}\sum_{pq}\left(-V_{pq}^{1,+1}T_{pq}^{1,-1} - V_{pq}^{1,-1}T_{pq}^{1,+1} + V_{pq}^{1,0}T_{pq}^{1,0}\right). \quad (1)$$

For spin-forbidden transitions involving a singlet and a triplet state, the three components of the triplet state can couple to the singlet state through the three components of the SOC operator.

$$\left\langle {}^1 0 \middle| V^{\mathrm{SOC}} \middle| {}^{3,m_s} f \right\rangle = \begin{cases} -\frac{1}{2}\sum_{pq} V_{pq}^{1,+1}\left\langle {}^1 0 \middle| T_{pq}^{1,-1} \middle| {}^{3,+1} f \right\rangle \\ -\frac{1}{2}\sum_{pq} V_{pq}^{1,-1}\left\langle {}^1 0 \middle| T_{pq}^{1,+1} \middle| {}^{3,-1} f \right\rangle \\ +\frac{1}{2}\sum_{pq} V_{pq}^{1,0}\left\langle {}^1 0 \middle| T_{pq}^{1,0} \middle| {}^{3,0} f \right\rangle \end{cases} \quad (2)$$

The definitions of the symbols can be found in the ESI.† A formulation that requires only the $\langle {}^1 0 | T_{pq} | {}^{3,0} f \rangle$ matrix element of the T_{pq} operator can be found using the Wigner–Eckart theorem. This allows the treatment of singlet–triplet transitions in a spin-free formalism[17] without generating the $M_s = +1$ and $M_s = -1$ components of the triplet state. For the oscillator strengths, one obtains as final result that the summation over the components of the triplet state is replaced by a summation of the three Cartesian components of the SOC operator, with all expressions evaluated for the $M_s = 0$ component of the triplet state.[17] It was further verified that the spin-free formulation obtained from the Wigner–Eckart theorem for the spin-forbidden oscillator strengths is also valid for the rotational strengths. For a detailed proof, we refer to the ESI.†

2.1 Work protocol for spin-forbidden rotational strengths

The CPP rotational strengths were computed with the TURBOMOLE[22] package as an extension of the phosphorescence lifetime code which was implemented in a preceding work into the RI-CC2 program[17] ricc2 and uses SOC-PT within the framework of CC response theory.

Published on 26 July 2018. Downloaded by Ruhr Universitat Bochum on 12/22/2018 1:42:38 PM.

Because of the non-Hermitian structure of coupled cluster theory, the left and right transition moments are not adjoints of each other *i.e.* $T_{0f}^{x} \neq (T_{f0}^{x})^{*}$ and are computed separately. As a consequence, a symmetrisation with respect to an interchange of the operators X and Y is required[17] for the transition strengths:

$$S_{XY}^{0f} = \langle 0|X|f\rangle\langle f|Y|0\rangle = \frac{1}{2}\left[T_{0f}^{X}T_{f0}^{Y} + \left(T_{0f}^{Y}T_{f0}^{X}\right)^{*}\right] \quad (3)$$

The spin-forbidden transition moments are obtained by SOC-PT within the CC response theory framework. The working expression for the lowest-order SOC-induced transition strength, where the summation over the three M_s components of the triplet state, eqn (2), has been replaced by a summation over the three Cartesian components of the effective mean-field one-electron spin–orbit coupling operator V^{SOC} is:

$$\langle 0|X|f\rangle^{(1)}\langle f|Y|0\rangle^{(1)} = \frac{1}{2}\sum_{\alpha=x,y,z}\left[T_{0f}^{X,\alpha}T_{f0}^{Y,\alpha} + \left(T_{0f}^{Y,\alpha}T_{f0}^{X,\alpha}\right)^{*}\right], \quad (4)$$

where $T_{0f}^{X,\alpha}$ and $T_{f0}^{X,\alpha}$ denote the transitions moments induced in first-order by the Cartesian component α of V^{SOC}.

2.1.1 Rotational strength in velocity gauge formulation. In the velocity gauge the rotational strength[8,9] for a transition between the ground state $|0\rangle$ and an excited state $|f\rangle$ is obtained as:

$${}^{f}R^{v} = \frac{1}{2\omega_f}\langle 0|\mathbf{p}|f\rangle \cdot \langle f|\mathbf{L}|0\rangle. \quad (5)$$

In the last equation **p** is the vector with the linear momentum and **L** the vector with the angular momentum operators, and ω_n is the excitation energy. The working expression for the spin-forbidden rotational strength including the summation over the three Cartesian components of V^{SOC} in the velocity gauge formulation is:

$$\langle 0|\mathbf{p}|f\rangle^{(1)}\langle 0|\mathbf{L}|f\rangle^{(1)} = \frac{1}{2}\sum_{\alpha=x,y,z}\sum_{\beta=x,y,z}\left[T_{0f}^{p_\beta,\alpha}T_{f0}^{L_\beta,\alpha} + \left(T_{0f}^{L_\beta,\alpha}T_{f0}^{p_\beta,\alpha}\right)^{*}\right] \quad (6)$$

2.1.2 Rotational strength in length gauge formulation. In the length gauge the rotational strength[8,9] is expressed through the transition moments of the position (**r**) and angular momentum (**L**) operators.

$${}^{f}R^{r} = -\frac{i}{2}\langle 0|\mathbf{r}|f\rangle \cdot \langle f|\mathbf{L}|0\rangle \quad (7)$$

The working expression for the spin-forbidden rotational strength with the summation over the three Cartesian components of V^{SOC} in the length gauge formulation is:

$$\langle 0|\mathbf{r}|f\rangle^{(1)}\langle 0|\mathbf{L}|f\rangle^{(1)} = \frac{1}{2}\sum_{\alpha=x,y,z}\sum_{\beta=x,y,z}\left[T_{0f}^{r_\beta,\alpha}T_{f0}^{L_\beta,\alpha} + \left(T_{0f}^{L_\beta,\alpha}T_{f0}^{r_\beta,\alpha}\right)^{*}\right] \quad (8)$$

If the magnetic dipole operator is represented in standard atom-centered atomic orbitals as, $\mathbf{B} = \frac{1}{2}\mathbf{L}$, *i.e.* if not gauge-including atomic orbitals are used, coupled cluster response calculations give in general only with the velocity gauge formulation gauge origin-independent results.[10]

2.2 Dipole strength

The absorption intensity for a transition from the ground state $|0\rangle$ to the excited state $|n\rangle$ is proportional to the scalar dipole strength and is in the velocity and length gauge given by,[8] respectively:

$${}^{n}D^{v} = \frac{1}{\omega_n{}^{2}}\langle 0|\mathbf{p}|n\rangle \cdot \langle n|\mathbf{p}|0\rangle, \quad (9)$$

$${}^{n}D^{r} = \langle 0|\mathbf{r}|n\rangle \cdot \langle n|\mathbf{r}|0\rangle. \quad (10)$$

3 Computational details

3.1 Choice of molecules

The chiral ketones (molecules **1–7**) shown in Fig. 1 were taken from ref. 8 and 11 where DFT results were reported for CD, CPL and CPP.

Furthermore, to show the applicability of SOC-PT-CC2 to larger experimentally relevant systems, a metal-free chiral aromatic system (structure **8**) shown in Fig. 2, which exhibits CPP, CPF and CD at room temperature,[21] has been studied.

3.2 Basis sets and methods

For all calculations reported below we used the correlation consistent cc-pVTZ,[23] aug-cc-pVXZ and d-aug-cc-pVXZ basis sets[24] with X = D, T, Q. The ground state DFT geometry optimisations were done with the B3LYP[25,26] functional for small molecules (molecules **1–7**) and the dispersion-corrected[27] B3LYP-D3 functional for the larger *N*,*N*′-dimethyl-1,1′-binaphthyldiamine (DMBDA) system (structure **8**).

A development version of the TURBOMOLE[28] package was used to compute the spin-forbidden transition moments. All other

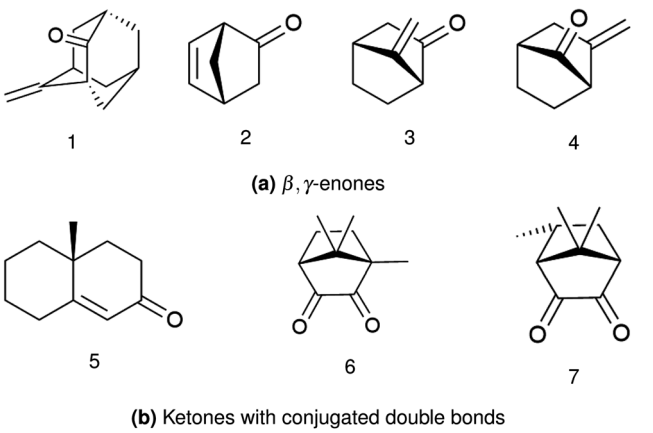
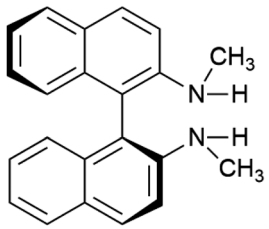


Fig. 1 Lewis structures of the β,γ-enones and conjugated ketones studied in Sections 4.3 and 4.4: (1*S*,3*R*)-4-methyleneadamantan-2-one **1**, (1*R*,4*R*)-bicyclo[2.2.1]hept-5-en-2-one **2**, (1*R*)-7-methylenebicyclo[2.2.1]heptan-2-one **3**, (1*S*)-2-methylenebicyclo[2.2.1]heptan-7-one **4**, (*R*)-(−)4,4*a*,5,6,7,8-hexahydro-4*a*-methyl-2(3*H*)-naphthalenone **5**, (1*S*,4*R*)-1,7,7-trimethylbicyclo-[2.2.1]heptane-2,3-dione (camphorquinone, **6**), (1*S*,4*R*,5*R*)-5,7,7 trimethyl-bicyclo[2.2.1]heptane-2,3-dione **7**.

Published on 26 July 2018. Downloaded by Ruhr Universitat Bochum on 12/22/2018 1:42:38 PM.



8

Fig. 2 Lewis structure of metal-free chiral aromatic system studied in Section 4.5: (*S*)-DMBDA ((*S*)-*N*,*N*′-dimethyl-1,1′-binaphthyldiamine) **8**.

calculations were performed using TURBOMOLE V7.1.[22] The two-component relativistic calculations X2C-HF-SCF and X2C-CC2 were carried out using the ridft[29,30] and ricc2[31,32] programs, respectively. Point-charge nuclei have been used for all calculations. The non-relativistic calculations were done with the dscf[33] and ricc2[32] programs.

For the RI approximation the corresponding optimised auxiliary basis sets[34,35] were used. The frozen-core approximation was used for all non-valence electrons in the correlation and response treatment. A numerical Laplace transformation was used for the one-electron density matrices that involve derivatives of the cluster amplitude or eigen vectors.[17] The convergence threshold for the numerical Laplace transformation was set to 10^{-6}.

4 Results and discussion

4.1 Test calculations on H_2O_2

A small computational model, H_2O_2 in only one of its chiral ground state minima, was used to test the correctness of the implementation and the basis set convergence. For these calculations we used the DFT-optimised ground state structure. In order to check the correctness of the SOC-PT implementation, X2C-CC2 calculations were the method of choice to check the SOC-PT-CC2 spin-forbidden rotational strengths of the test molecule.

The SOC-PT-CC2 calculation was compared with the relativistic 2-component calculation, which includes the SOC already at the SCF level. In the X2C calculation, only the one-electron part of the spin–orbit Hamiltonian is included. In the non-relativistic calculation, the coupling between the singlet and triplet states is described by a spin–orbit mean-field (SOMF) operator with matrix elements that include the one-electron and an effective two-electron contribution together with the spin-averaged HF-SCF density matrix as described in ref. 17. For a better comparison with the 2-component calculations we disabled the 2-electron contribution of the SOMF operator in the non-relativistic calculation. For the cc-pVTZ basis set, the agreement of the relativistic calculation with the perturbative calculation is for the rotational strength as good as for the oscillator strength (cmp. Table 1).

To verify the gauge-origin invariance of the velocity gauge results, we have done calculations in both the velocity and length gauge formulations for the transitions into the three lowest triplet states. Two sets of calculations were performed. In one case, the gauge origin was placed at the centre of mass, which is the default in the ricc2 program, and in the other case the origin was displaced from the centre of mass by the vector (1 a.u., 1 a.u., 1 a.u.). The HF calculations were done with a SCF convergence criterion of 10^{-12} a.u. for the energy and 10^{-7} for the one-electron density and used the same molecular orbitals for both the shifted and unshifted coordinates. The length and velocity gauge results are listed in Table 2. The length gauge results are origin dependent as expected. For the velocity-gauge results we observe only tiny variations in the fifth non-zero digit which are artefacts of remaining numerical noise. This demonstrates that with the velocity-gauge formulation also coupled-cluster results for the lowest-order SOC-induced rotational strengths are in fact origin invariant. Since the rotational strength values are in the following sections reported only up to two decimal places, the velocity-gauge results are with the default thresholds (10^{-7} a.u. for the one-electron density) sufficiently converged and this set up was used for all forthcoming calculations.

Table 1 Transition strengths (in a.u.) from X2C-CC2 and SOC-PT-CC2 for H_2O_2 method

	Oscillator strength		Rotational strength
	Velocity	Length	Velocity
X2C-CC2	1.68×10^{-6}	2.55×10^{-6}	-4.40×10^{-7}
CC2	2.40×10^{-6}	2.82×10^{-6}	-5.47×10^{-7}

The basis set dependence was studied for the lowest triplet state at the CC2-optimised ground state geometry. The results for various basis sets are listed in Table 3. We observe for the rotational strength a slightly faster convergence than for the dipole strength in the velocity gauge. Double augmentation does not change the results significantly. Since in the following we aim only at a semi-quantitative accuracy and study only excited states reached by valence transitions, we conclude that the aug-cc-pVDZ basis set provides sufficient accuracy for the rotational strengths. This basis was used to determine the rotational strengths for all molecules in the following sections.

4.2 Ground and excited state structures

The equilibrium geometries of the ground state and the excited state are important for determining rotational strengths of CD and CPL, respectively. When the two structures are similar, the emission and absorption bands have the same sign and similar magnitude, because the rotational strengths are then similar.[8] But, when the molecular structure is flexible enough and the excited state has a lifetime long enough to structurally relax, the CD and CPL bands can be quite different.

We first tested for a few examples if the results are sensitive whether DFT or CC2 is used for the optimisation of the ground state structures. The CD rotational strengths did not vary much between the CC2 and the DFT structures. For example, the spin-forbidden rotational strengths calculated with CC2/aug-cc-pVDZ for the first excited triplet state to ground state transition of enone **5** is 6.795×10^{-44} esu cm erg G^{-1} and 6.791×10^{-44} esu cm erg G^{-1} at,

 This journal is © the Owner Societies 2018

Published on 26 July 2018. Downloaded by Ruhr Universitat Bochum on 12/22/2018 1:42:38 PM.

Table 2 Gauge-origin dependence of rotational[esu cm erg G^{-1}] strengths in length and velocity gauge formulations for the first, second and third transitions in H_2O_2. CM refers to calculations with the gauge origin placed in the centre of mass, and CM + 1 where it is displaced by the vector (1 a.u., 1 a.u., 1 a.u.)

	Length		Velocity	
Basis set	CM	CM + 1	CM	CM + 1
aug-cc-pVQZ	-8.12991×10^{-46}	-1.85045×10^{-46}	-1.43551×10^{-44}	-1.43551×10^{-44}
aug-cc-Pvqz	-8.31087×10^{-44}	-8.34042×10^{-44}	-6.79695×10^{-4}	-6.79694×10^{-42}
aug-cc-pVQZ	-8.56312×10^{-46}	-7.23529×10^{-46}	1.35723×10^{-44}	1.35722×10^{-44}

Table 3 Basis set convergence of the velocity (D^v, R^v) and length (D^l) gauge results for the dipole [10^{-41} esu^2 cm^2] and rotational [10^{-45} esu cm erg G^{-1}] strengths for the lowest triplet transition in H_2O_2 for the CC2-optimised ground state structure with different basis sets

Basis set	D^l	D^v	R^v
aug-cc-pVDZ	8.37	5.10	−9.80
aug-cc-pVTZ	9.38	6.74	−8.86
aug-cc-pVQZ	9.70	7.54	−8.31
d-aug-cc-pVDZ	8.39	5.02	−8.91
d-aug-cc-pVTZ	9.39	6.75	−8.83
d-aug-cc-pVQZ	9.69	7.56	−8.31

respectively, the CC2 and the DFT geometry. For all further calculations we used therefore ground state geometries optimised at the DFT/B3LYP/cc-pVTZ level. The excited state geometries were optimised at the CC2/aug-cc-pVDZ level.

4.3 β,γ-Enones

CPL spectra with different signs have been predicted for some β,γ-enones for spin-allowed transitions based on DFT calculations.[8] This was attributed to the pyramidalisation of the carbonyl group in the excited state either towards or away from the C═C double bond causing an inversion in sign of CPL with respect to CD. Recently, similar sign inversions have also been predicted for CPP based on (TD)DFT calculations.[11] With the SOC-PT-CC2 implementation it became now possible to check with a correlated wavefunction method if it corroborates the TDDFT results.

For the enones **1–4** the carbonyl group is in the ground state coplanar with the two neighbouring C–C bonds, but in the excited state they are tilted out of this plane. This gives rise to two minima that differ in the tilting direction (cmp. Fig. 3). The CC2 results for the CPF (cmp. Table 4) compare in most cases well with the DFT results from ref. 8. With CC2 we also found for enone **2** both minima on the S_1 surface while at the TDDFT level in ref. 8 only one minimum was found. Another difference is that for enone **3** CC2 did not give a sign change from the GS to the S1b structure as predicted by the DFT results from ref. 8. This is possibly due to an exchange of close lying excited states between DFT and CC2.

The most dominant natural transition orbitals[36] (NTOs) for the S_1 to GS transitions are shown in Fig. 4. At the CC2 level the excitation to S_1 is for all four enones at both excited state minima dominated by the n → π* transition in the carbonyl group. CC2 gives in the S_1 states longer carbonyl bond lengths compared to the TDDFT calculations[8] and typically overestimates them also compared to experiment,[37] which may be a reason for the differences in the results.

The DFT results for CPF showed that the rotational strength is sensitive to geometric parameters such as dihedral angles and bond lengths of the chromophores. For the enones **2** and **3**, where the CPL does not change its sign between the two minima on the S_1 surface, the NTOs appear to be more similar for both structures than for the enones **1** and **4**. Since the NTOs are related to the transition moments which are used to calculate the rotational strengths similar NTOs imply qualitatively similar transition moments. The rotational strengths should be similar if the NTOs are similar. The orbitals involved in the n → π* excitation are to some extent delocalised on the C═C bond as hypothesised in ref. 8.

We have then optimised equilibrium structures for the lowest triplet states and computed the rotational strength for the circularly polarised phosphorescence with SOC-PT. The energies for the lowest transitions are compiled in Table 5, the results are summarised in Table 6. In all cases, the CPP rotational strengths are at least four orders of magnitude smaller than the CPF rotational strengths for the corresponding excited singlet state. The CC2 results for the CPP rotational strengths agree in most cases qualitatively with those from TDDFT.[11] There are, however, some exceptions: for enone **1** and enone **4** CC2 does not predict opposite signs for the CPP from the two T_1 minima. For enone **2** the CC2 results for the spin-forbidden rotational strengths have for all cases the opposite sign of the respective DFT results. This is possibly due to an exchange of order between close-lying excited states between DFT and CC2. The NTO analysis (cmp. Fig. 5) reveals that at the T1a minimum of enone **2** the transition to T_1 is in the CC2 calculations a ππ* excitation in the C═C group.

In general, the equilibrium structures on the T_1 surface are similar to the respective minima on the S_1 surface with a pyramidalisation of the carbonyl group. The NTOs show that for these molecules also the lowest triplet excitation is a n → π* transition in the carbonyl group except for the T1a minimum of enone **2**. When the structures of the ground and the excited state are similar, also the signs of the rotational strengths are similar.

4.4 Ketones with conjugated double bonds

Next we studied the three ketones **5–7** (see Fig. 6) with conjugated doubles bonds, which have more rigid structures. The results for the α,β-enone **5** are summarised in Table 7 (note that for this molecule the DFT calculations in ref. 11 were done for the other enantiomer). The CC2 results for the CD compare well with DFT, but the CPP result for the first excited triplet state has the opposite sign of the respective DFT result.

Published on 26 July 2018. Downloaded by Ruhr Universitat Bochum on 12/22/2018 1:42:38 PM.

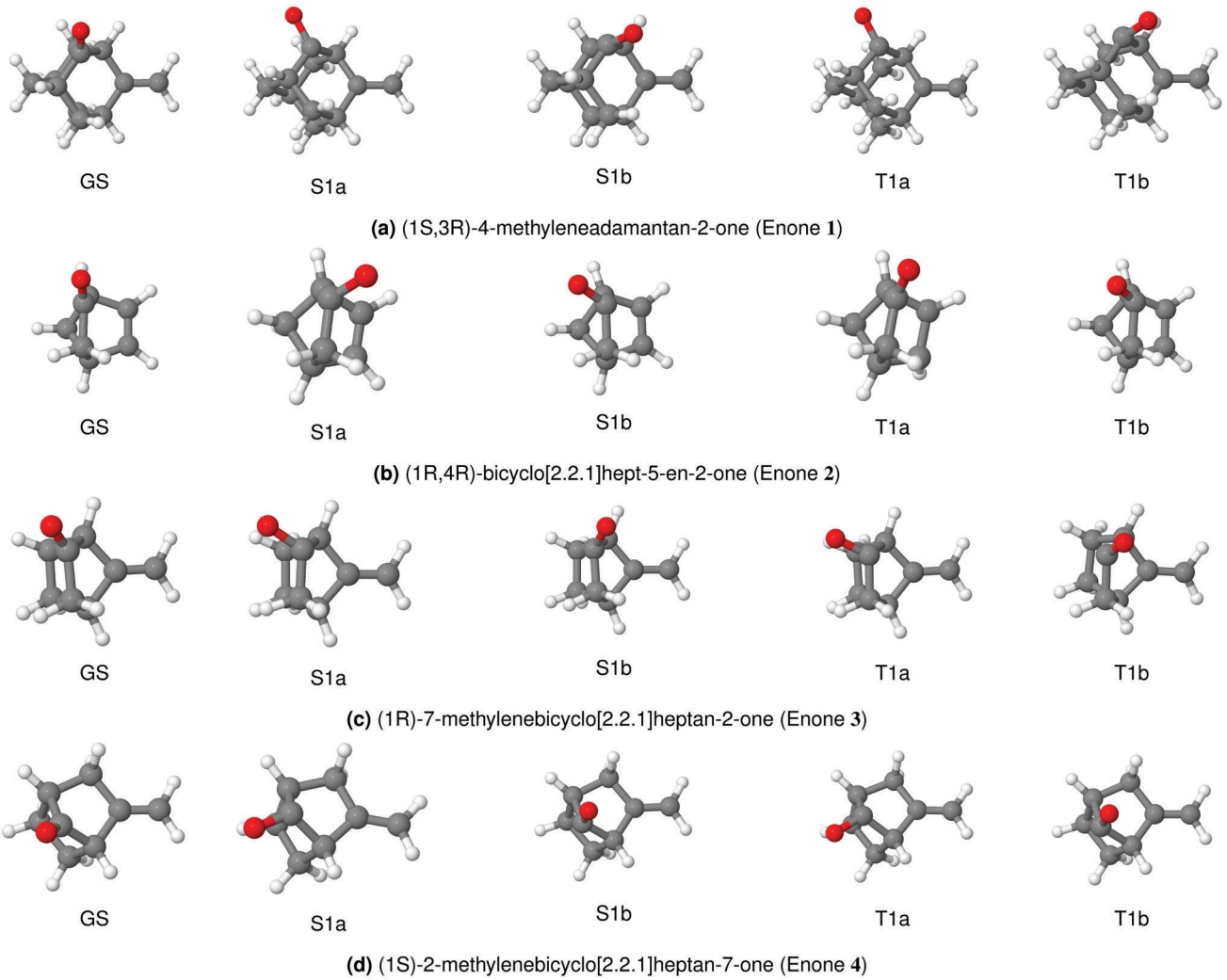


Fig. 3 The ground and first excited state structures of enones **1–4**. GS refers to the ground state structure, S1a, S1b refer to the two possible first excited singlet state structures and T1a, T1b refer to the two possible first excited triplet state structures respectively.

Table 4 Rotational strengths [esu cm erg G^{-1}] in velocity gauge for singlet–singlet transitions in enones obtained with CC2/aug-cc-pVDZ. GS refers to the ground state structure, S1a and S1b refer to the two conformers on the S_1 surface. The DFT results from ref. 8 are given in parentheses for comparison

Strength	GS	S1a	S1b
Enone 1	1.20×10^{-39} (8.54×10^{-40})	3.15×10^{-40} (5.72×10^{-40})	-1.23×10^{40} (-9.86×10^{-40})
Enone 2	4.25×10^{-39} (4.57×10^{-39})	1.26×10^{-39}	3.96×10^{-40} (3.09×10^{-39})
Enone 3	2.34×10^{-39} (2.19×10^{-39})	5.08×10^{-40} (1.34×10^{-39})	6.56×10^{-40} (-1.62×10^{-40})
Enone 4	-2.03×10^{-39} (-1.86×10^{-39})	-5.80×10^{-40} (-9.19×10^{-40})	1.95×10^{-41} (3.30×10^{-40})

This could be because of an exchange of states between DFT and CC2. The second excited state in absorption is only 0.5 eV higher making this not unlikely.

For the diketones **6** and **7** we included in the study the lowest three singlet and triplet excited states. The results for CD and CPL are tabulated for both the spin-allowed and the spin-forbidden transitions in Table 8. One would expect that the sign of the rotational strength is the same in CD and CPL. But this is not true for all cases. However, as can be seen from the transition energies compiled in Table 9 the deexcitation energies differ by more than 1 eV from the respective excitation energies which indicates significant relaxations of the molecular and electronic structures. The character of the transitions at the equilibrium structures of the triplet excited states of enone **6** are depicted in Fig. 7. Also, since no pyramidalisation of the carbonyl groups happens in the excited states, it is clear that pyramidalisation is not the only reason for sign change in CD and CPL.

It is also seen that the absolute value of the rotational strength for the third excited state is always higher than for the first two excited states. In some cases it is one or two orders of magnitude higher. This is possibly due to higher asymmetry

 This journal is © the Owner Societies 2018

Published on 26 July 2018. Downloaded by Ruhr Universitat Bochum on 12/22/2018 1:42:38 PM.

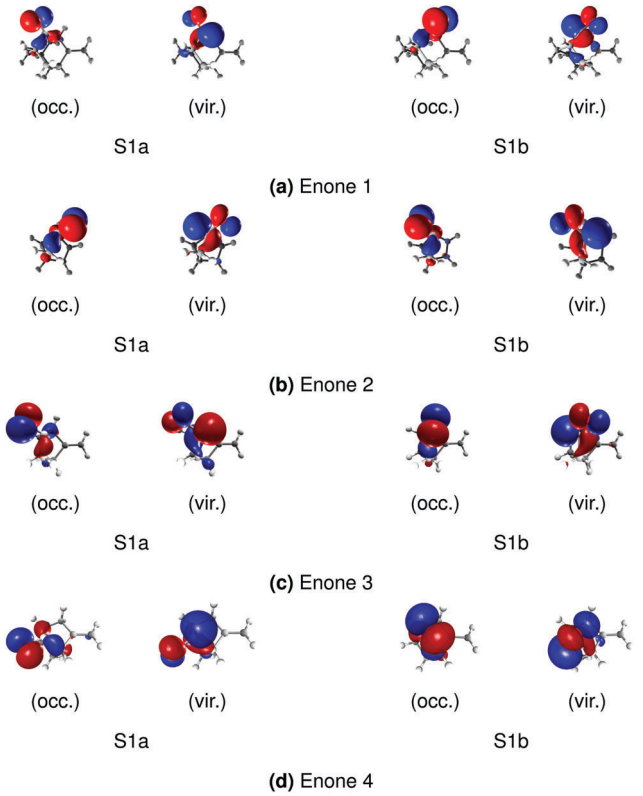


Fig. 4 Most dominant occupied (occ.) and virtual (vir.) natural transition orbitals of enones **1–4** for the lowest singlet excitation at the excited state structures. The NTOs show that S_1 is in all cases the n → π* excitation at the keto group.

Table 5 Vertical transition energies for CD, CPF and CPP for transitions between ground and first excited state ΔE (eV)

	Gr → T_1	T1a	T1b	Gr → S_1	S1a	S1b
Enone 1	3.95	2.05	2.05	4.35	2.41	2.45
Enone 2	3.85	1.04	1.93	4.30	2.54	2.44
Enone 3	3.81	2.08	2.06	4.17	2.50	2.55
Enone 4	3.96	1.80	1.79	4.37	2.35	2.36

of the occupied NTO for the π → π* transitions that can be observed in Fig. 7.

4.5 CPP in (*S*)-DMBDA

The combination with the RI approximation and the perturbative treatment of the spin–orbit coupling makes is possible to compute also for larger molecules rotational strengths for spin-forbidden transitions at the CC2 level. As an example we present an application to a metal-free chiral aromatic system (44 atoms), (*S*)-DMBDA ((*S*)-*N*,*N*′-dimethyl-1,1′-binaphthyldiamine), which exhibits a circularly-polarised persistent room-temperature phosphorescence.[21]

In a recent DFT study Hirata and Vacha found for the ωB97XD functional and the cc-pVTZ basis both on the ground state and on the S_1 surface of (*S*)-DMBDA three conformeric minima, which differ in the orientation of the methyl-amino groups and the dihedral angle between the two binaphthyl rings.

Table 6 Rotational strengths [esu cm erg G^{-1}] in velocity gauge for singlet–triplet transitions in the enones at the CC2/aug-cc-pVDZ level. GS refers to the ground state structure, T1a and T1b to the two conformers on the T_1 surface. The DFT results from ref. 11 for rotational strengths are given in parentheses for comparison

	GS	T1a	T1b
Enone 1			
R	-3.43×10^{-45} (-2.53×10^{-44})	-6.27×10^{-45} (2.52×10^{-42})	-6.56×10^{-45} (-6.93×10^{-44})
Enone 2			
R	-1.00×10^{-44} (2.32×10^{-45})	1.70×10^{-45} (-1.99×10^{-44})	-9.71×10^{-46} (5.72×10^{-45})
Enone 3			
R	6.87×10^{-45} (1.68×10^{-44})	2.05×10^{-44} (5.75×10^{-44})	-8.64×10^{-45} (1.68×10^{-44})
Enone 4			
R	8.43×10^{-47} (2.32×10^{-45})	3.64×10^{-45} (-1.99×10^{-44})	1.74×10^{-45} (5.72×10^{-45})

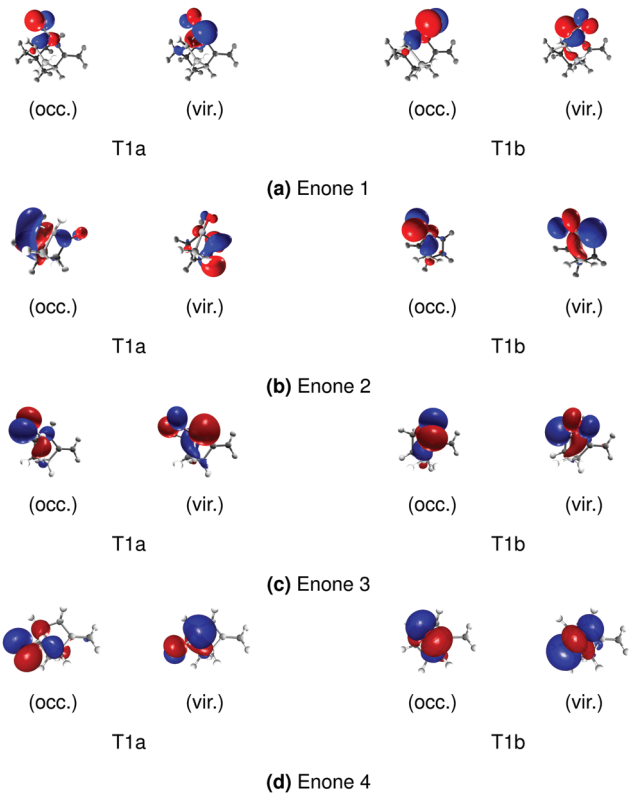


Fig. 5 Most dominant occupied (occ.) and virtual (vir.) natural transition orbitals of enones **1–4** for the lowest triplet excitation at the excited state structures.

The relative energies of the conformers are given in Table 11. In addition they determined one minimum on the T_1 surface. In the current study we used DFT/B3LYP-D3/cc-pVTZ for the ground state and CC2/aug-cc-pVDZ for the excited state geometry optimisations. In both cases, S_0 and S_1, we could only locate two minima and also on the triplet surface we also found two minima (T_1 and T_1'). The CC2 excited state geometries agree

Published on 26 July 2018. Downloaded by Ruhr Universitat Bochum on 12/22/2018 1:42:38 PM.

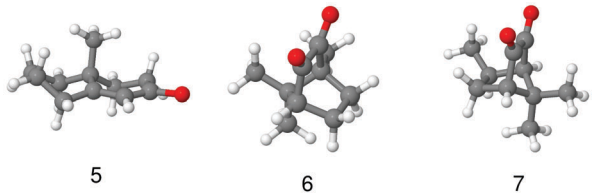


Fig. 6 The T_1 equilibrium structures of the α,β-enone **5** and the diketones **6** and **7**.

Table 7 The rotational strengths [esu cm erg G^{-1}] in velocity gauge for transitions to S_1 and T_1 in enone **5** at the ground state (absorption) and at the S_1 and T_1 (emission) structure with CC2/aug-cc-pVDZ. The DFT results from ref. 11 for rotational strengths are given in parentheses for comparison

	S_1	T_1
Absorption	-5.71×10^{-40}	6.79×10^{-44} (-3.37×10^{-43})
Emission	-4.00×10^{-40}	2.47×10^{-43} (4.31×10^{-43})

well with those from DFT in most cases. The calculations for rotational strengths for CPL and CD were again done at the CC2/aug-cc-pVDZ level. The results for the (*S*)-DMBDA enantiomer are summarised the Table 10. For the singlet transitions they agree qualitatively with the TDDFT results from ref. 21. Fig. 8 also shows the optimised geometries for the triplet excited state at the CC2/aug-cc-pVDZ level. For the spin-forbidden ($T_1 \rightarrow S_0$ and $T_1' \rightarrow S_0'$) transitions in DMBDA no theoretical values have been obtained before. The CC2 calculations give for this transition a rotational strength which has the same sign as for the CD and the CPF of the S_0 and S_1 conformers with a similar structure, which is in agreement with the experimental results in ref. 21.

The NTOs for the singlet–singlet transitions for one of the conformers show charge-transfer from one naphthyl group to the other. If DMBDA would be C_2-symmetric another set of NTOs with a charge-transfer between the naphthyls in the opposite direction should contribute with an equal weight to the transition. The symmetry breaking induced by the methyl groups leads for (*S*)-DMBDA to a localisation of the charge transfer states; only one dominant NTO pair contributes to S_1. The charge transfer excitation in the opposite direction appears as S_2 at a only slightly higher excitation energy (3.73 instead of 3.67 eV in CC2, cmp. Table 10). This transition is connected with a rotational strength which has the opposite sign. The presence of such a close-lying excited state with an opposite sign for the rotational strength becomes important when comparing results with other methods or experiment. For the S_0' conformer the $S_0 \rightarrow S_1$ transition is a local excitation in one of the naphthyl groups. In this case, we also find that the rotational strengths for CD and CPL have opposite signs.

The rotational strength calculated for the spin-forbidden triplet to singlet transition with SOC-PT-CC2 is 5.96×10^{-47} esu cm erg G^{-1}. Experimentally, the phosphorescence is observed between 500–600 nm which agrees well with our result at ≈556 nm corresponding to the yellow region of the visible spectrum. Its sign agrees with the experimentally observed sign of the Cotton effect. The NTOs (see Fig. 9) for this transition show that this transition is local excitation in one of the naphthyl groups. The results for the second triplet conformer, not found in the DFT study, is also included in Tables 10 and 11. The NTOs reveal that also this transition is a local excitation in one of the naphthyl groups (cmp. Fig. 9).

5 Summary and conclusions

A computational protocol for dipole and rotational strengths of spin-forbidden CD and CPP where the spin–orbit coupling is treated as a perturbation (SOC-PT) for the non-relativistic Hamiltonian has been established for CC response theory and implemented for the approximate singles and doubles model CC2. A spin-free formalism was used to treat the singlet–triplet transitions.[16,17] The SOC-PT approach is applicable for closed-shell molecules containing only light elements. It has been verified that the simplification obtained in the spin-free

Table 8 The rotational strengths [10^{-40} esu cm erg G^{-1}] in velocity gauge for CD, CPF and CPP transitions in diketones **6** and **7** using CC2/aug-cc-pVDZ. The DFT results from ref. 11 for rotational strengths are given in parentheses for comparison

Excited state	Absorption (CD)	Emission (CPL)	Excited state	Absorption (spin-forbidden CD)	Emission (CPP)
Diketone 6					
S_1	−1.01 (0.99)	1.13 (1.43)	T_1	2.75×10^{-6} (-1.30×10^{-6})	-7.52×10^{-6} (-3.10×10^{-6})
S_2	0.30 (−0.82)	−0.17 (−0.87)	T_2	2.53×10^{-5} (7.14×10^{-5})	1.34×10^{-5} (6.12×10^{-3})
S_3	13.84 (6.58)	26.56 (29.96)	T_3	-4.45×10^{-5} (-7.23×10^{-4})	-1.08×10^{-4} (-7.33×10^{-4})
Diketone 7					
S_1	−0.95 (−1.31)	−0.80 (−0.69)	T_1	5.45×10^{-6} (-1.68×10^{-5})	-1.08×10^{-5} (4.14×10^{-6})
S_2	0.70 (1.93)	0.39 (0.45)	T_2	1.76×10^{-5} (-1.49×10^{-5})	-8.55×10^{-5} (-1.27×10^{-4})
S_3	3.09 (−11.41)	−2.13 (0.97)	T_3	-3.69×10^{-5} (1.68×10^{-3})	9.55×10^{-5} (2.59×10^{-4})

 This journal is © the Owner Societies 2018

Published on 26 July 2018. Downloaded by Ruhr Universitat Bochum on 12/22/2018 1:42:38 PM.

Table 9 Vertical transition energies (in eV) between the ground and the first excited singlet and triplet states for the diketones **6** and **7** with CC2/aug-cc-pVDZ. In the right most column n(s) and n(a) denote the symmetric and anti-symmetric linear combinations of the oxygen lone pairs

Excited state	Absorption	Emission	Excited state	Absorption	Emission	Character
Diketone 6						
S_1	3.82	2.29	T_1	2.94	1.95	$n(s) \rightarrow \pi^*$
S_2	4.93	2.62	T_2	4.09	2.28	$n(a) \rightarrow \pi^*$
S_3	5.91	4.49	T_3	4.11	3.07	$\pi \rightarrow \pi^*$
Diketone 7						
S_1	3.79	2.29	T_1	3.02	1.94	$n(s) \rightarrow \pi^*$
S_2	5.00	2.57	T_2	4.06	2.23	$n(a) \rightarrow \pi^*$
S_3	5.48	4.26	T_3	4.15	3.08	$\pi \rightarrow \pi^*$

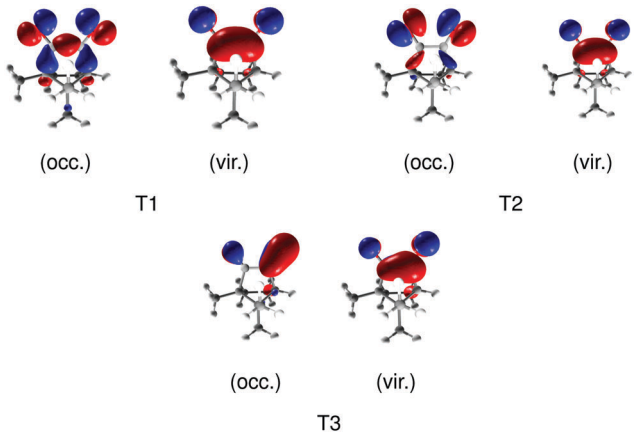


Fig. 7 Most dominant occupied (occ.) and virtual (vir.) natural transition orbitals at the triplet excited state structures of (1*S*,4*R*)-1,7,7-trimethylbicyclo[2.2.1]heptane-2,3-dione (camphorquinone, **6**).

Table 10 The dipole [esu^2 cm^2] and rotational strengths [esu cm erg G^{-1}] and transition energies ΔE [eV] of different transitions in (*S*)-DMBDA. The DFT results from ref. 21 for *R*-DMBDA are given in parentheses for comparison. (Note that *R*-DMBDA and *S*-DMBDA have opposite signs for rotational strengths)

Transition	D	R	ΔE	$\frac{R}{D}$
$S_0 \rightarrow S_1$	5.85×10^{-36}	2.81×10^{-39} (-1.20×10^{-38})	3.67	4.80×10^{-4}
$S_0' \rightarrow S_1'$	5.32×10^{-36}	5.96×10^{-39} (-4.91×10^{-40})	3.72	1.12×10^{-3}
$S_0 \rightarrow S_2$	3.86×10^{-36}	-5.62×10^{-39}	3.73	-1.46×10^{-3}
$S_1 \rightarrow S_0$	9.00×10^{-36}	5.85×10^{-39} (-1.05×10^{-38})	2.87	6.50×10^{-4}
$S_1' \rightarrow S_0'$	4.99×10^{-36}	-1.12×10^{-39} (2.23×10^{-39})	2.78	-2.24×10^{-4}
$T_1 \rightarrow S_0$	1.01×10^{-43}	5.96×10^{-47}	2.23	5.89×10^{-4}
$T_1' \rightarrow S_0'$	7.42×10^{-44}	1.10×10^{-46}	2.32	1.49×10^{-3}

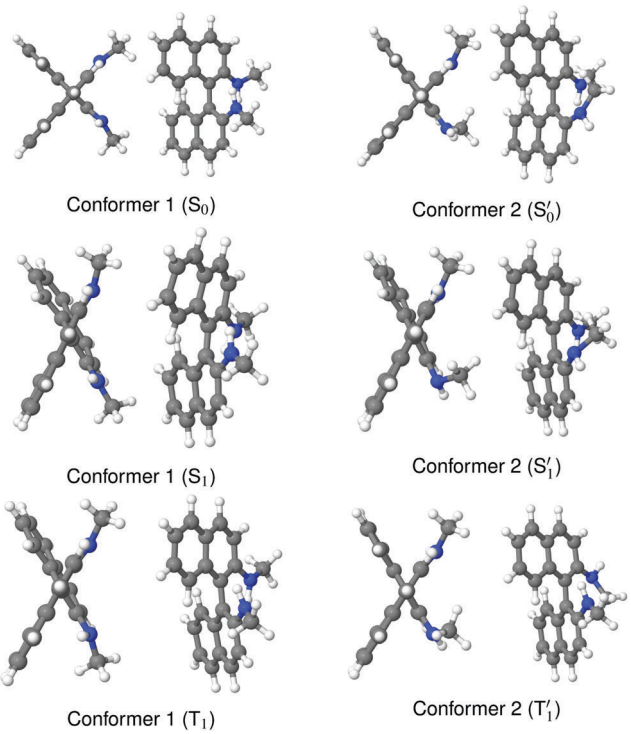


Fig. 8 The geometry-optimised ground state (S_0 and S_0'), first excited singlet state (S_1 and S_1') for two conformers and first excited triplet state for two conformers (T_1 and T_1') structures of (*S*)-DMBDA.

case from the Wigner–Eckhart theorem for the spin-forbidden oscillator strengths in phosphorescence[17] transfer to the pseudoscalar rotational strengths in spin-forbidden circularly polarised phosphorescence. The correctness of the implementation was tested by a comparison against relativistic two-component CC2 calculations within the X2C approach,[31] X2C-CC2, and by testing the gauge-origin invariance of the rotational strength in the velocity form. Furthermore we checked also at the CC2 level that the basis set dependence of the spin-forbidden rotational strengths is only week once the electronic transition is described qualitatively correct.

Applications are presented for β,γ-enones and ketones with conjugated double bonds, where literature results are available from earlier TDDFT calculations.[8] The CC2 calculations gave for the CD, CPF and CPP of the β,γ-enones and conjugated ketones rotational strengths which agree in most cases qualitatively with the results from the DFT calculations. In a few cases where the rotational strength differ in sign between the DFT and CC2 results, a switch between close-lying excited states between DFT and CC2 is not unlikely. The β,γ-enones exhibit two minima with similar energies ($\approx$0.05 eV) in the first excited singlet and triplet states. In some cases, the CC2 calculations

Published on 26 July 2018. Downloaded by Ruhr Universitat Bochum on 12/22/2018 1:42:38 PM.

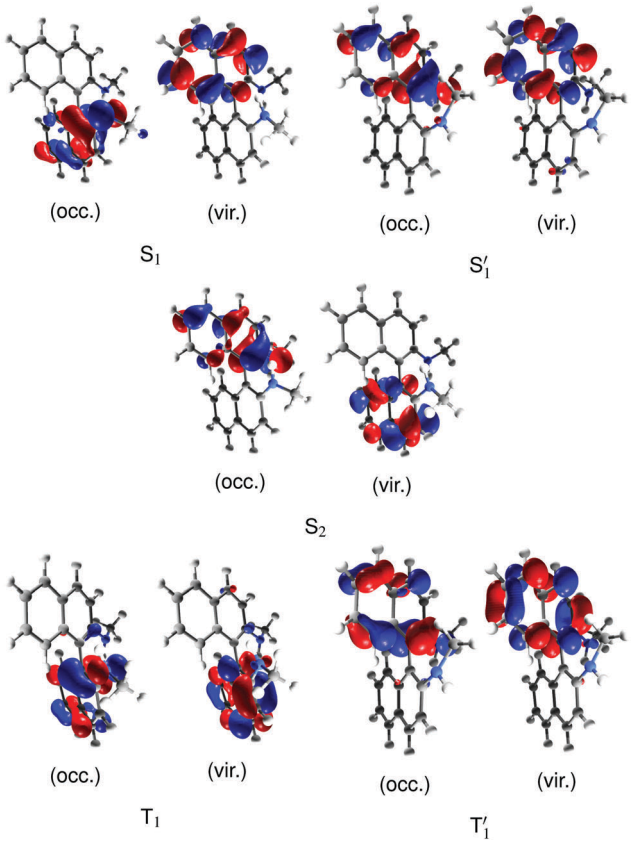


Fig. 9 Most dominant occupied (occ.) and virtual (vir.) natural transition orbitals of (*S*)-DMBDA for the transition from ground state to excited state as visualised on the ground state (S_0 and S_0') structures.

Table 11 The relative energies ΔE [eV] and dihedral angles [°] of different conformers in (*S*)-DMBDA. The DFT results from ref. 21 for *R*-DMBDA are given in parentheses for comparison

Transition	ΔE	Dihedral angles
S_0	0	92.3 (91.6)
S_0'	0.06	103.2 (77.3)
S_1	2.87	120.3 (121.5)
S_1'	2.84	121.7 (70.5)
T_1	2.23	116.1 (103.9)
T_1'	2.32	115.6

predict opposite signs for rotational strengths for the two minima which is related to the pyramidalisation of the carbonyl group in the excited state towards or away from the C═C double bond.

Since the SOC-PT-CC2 implementation uses the RI approximation for the electron repulsion integrals, it is also applicable to larger molecules. As an example we studied a molecule with 44 atoms, (*S*)-DMBDA, which was recently reported to exhibit circularly polarised persistent room-temperature phosphorescence.[21] Experimentally, the phosphorescence is observed between 500–600 nm which agrees well with our result at ≈556 nm. The rotational strength calculated for the spin-forbidden triplet–singlet transition for (*S*)-DMBDA is 5.96×10^{-47} esu cm erg G^{-1}. Its sign agrees with the experimentally observed sign of the Cotton effect.

Conflicts of interest

There are no conflicts to declare.

Acknowledgements

This work was supported by the Deutsche Forschungsgemeinschaft (DFG) through grant Ha 2588/5-2. The authors thank Sonia Coriani and the authors of ref. 11 for helpful discussions.

References

1 J. Hummelen, H. Wynberg, E. Meijer and H. Dekkers, *Nature*, 1980, 265.
2 B. N. Samoilov, *J. Exp. Theor. Phys.*, 1948, **18**, 1030–1040.
3 B. Pritchard and J. Autschbach, *ChemPhysChem*, 2010, **11**, 2409–2415.
4 J. Schlessinger and A. Warshel, *Chem. Phys. Lett.*, 1974, **28**, 380–383.
5 E. Anslyn and D. Dougherty, *Modern Physical Organic Chemistry*, University Science Books, 2006.
6 C. Emeis and L. Oosterhoff, *Chem. Phys. Lett.*, 1967, **1**, 129–132.
7 F. S. Richardson and J. P. Riehl, *Chem. Rev.*, 1977, **77**, 773–792.
8 M. Pecul and K. Ruud, *Phys. Chem. Chem. Phys.*, 2011, **13**, 643–650.
9 K. L. Bak, A. E. Hansen, K. Ruud, T. Helgaker, J. Olsen and P. Jørgensen, *Theor. Chim. Acta*, 1995, **90**, 441–458.
10 T. B. Pedersen, H. Koch and K. Ruud, *J. Chem. Phys.*, 1999, **110**, 2883–2892.
11 M. Kaminski, J. Cukras, M. Pecul, A. Rizzo and S. Coriani, *Phys. Chem. Chem. Phys.*, 2015, **17**, 19079–19086.
12 H. R. McAlexander and T. D. Crawford, *J. Chem. Phys.*, 2015, **142**, 154101.
13 G. Longhi, E. Castiglioni, J. Koshoubu, G. Mazzeo and S. Abbate, *Chirality*, 2016, **28**, 696–707.
14 K. G. Dyall, *J. Chem. Phys.*, 1997, **106**, 9618–9626.
15 W. Kutzelnigg and W. Liu, *J. Chem. Phys.*, 2005, **123**, 241102.
16 C. Hättig, A. Köhn and K. Hald, *J. Chem. Phys.*, 2002, **116**, 5401–5410.
17 B. Helmich-Paris, C. Hättig and C. van Wüllen, *J. Chem. Theory Comput.*, 2016, **12**, 1892–1904.
18 O. Vahtras, H. Agren, P. Jørgensen, H. J. A. Jensen, T. Helgaker and J. Olsen, *J. Chem. Phys.*, 1992, **97**, 9178–9187.
19 O. Christiansen, J. Gauss and B. Schimmelpfennig, *Phys. Chem. Chem. Phys.*, 2000, **2**, 965–971.

 This journal is © the Owner Societies 2018

Published on 26 July 2018. Downloaded by Ruhr Universitat Bochum on 12/22/2018 1:42:38 PM.

20 T. B. Pedersen and A. E. Hansen, *Chem. Phys. Lett.*, 1995, **246**, 1–8.
21 S. Hirata and M. Vacha, *J. Phys. Chem. Lett.*, 2016, **7**, 1539–1545.
22 TURBOMOLE V7.1 2015, a development of University of Karlsruhe and Forschungszentrum Karlsruhe GmbH, 1989–2007, TURBOMOLE GmbH, since 2007; available from http://www.turbomole.com.
23 T. H. Dunning, *J. Chem. Phys.*, 1989, **90**, 1007–1023.
24 R. A. Kendall, T. H. Dunning and R. J. Harrison, *J. Chem. Phys.*, 1992, **96**, 6796–6806.
25 C. Lee, W. Yang and R. G. Parr, *Phys. Rev. B: Condens. Matter Mater. Phys.*, 1988, **37**, 785–789.
26 A. D. Becke, *J. Chem. Phys.*, 1993, **98**, 5648–5652.
27 S. Grimme, *J. Comput. Chem.*, 2006, **27**, 1787–1799.
28 TURBOMOLE, development version, 2015; for further information see http://www.turbomole.com.
29 D. Peng, N. Middendorf, F. Weigend and M. Reiher, *J. Chem. Phys.*, 2013, **138**, 184105.
30 K. Eichkorn, O. Treutler, H. Öhm, M. Häser and R. Ahlrichs, *Chem. Phys. Lett.*, 1995, **240**, 283–290.
31 K. Krause and W. Klopper, *J. Chem. Phys.*, 2015, **142**, 104109.
32 C. Hättig and F. Weigend, *J. Chem. Phys.*, 2000, **113**, 5154–5161.
33 M. Häser and R. Ahlrichs, *J. Comput. Chem.*, 1989, **10**, 104–111.
34 F. Weigend, A. Köhn and C. Hättig, *J. Chem. Phys.*, 2002, **116**, 3175–3183.
35 F. Weigend, *J. Comput. Chem.*, 2008, **29**, 167–175.
36 R. L. Martin, *J. Chem. Phys.*, 2003, **118**, 4775–4777.
37 A. Köhn and C. Hättig, *J. Chem. Phys.*, 2003, **119**, 5021–5036.